A Novel Discrete Variable Stiffness Gripper Based on the Fin Ray Effect

Jiaming Fu[1], Han Lin[1], I. V. S. Prathyush[2], Xiaotong Huang[1], Lianxi Zheng[3], and Dongming Gan[1(✉)]

[1] Purdue University, West Lafayette, IN 47907, USA
dgan@purdue.edu
[2] Birla Institute of Technology and Science, Pilani 333031, India
[3] Khalifa University, Abu Dhabi 127788, UAE

Abstract. Variable stiffness grippers can adapt to objects with different shapes and gripping forces. This paper presents a novel variable stiffness gripper (VSG) based on the Fin Ray effect that can adjust stiffness discretely. The main structure of the gripper includes the compliant frame, rotatable ribs, and the position limit components attached to the compliant frame. The stiffness of the gripper can be adjusted by rotating the specific ribs in the frame. There are four configurations for the gripper that were developed in this research: a) all ribs OFF (Flex) mode; b) upper ribs ON and lower ribs OFF (Hold) mode; c) upper ribs OFF and lower ribs ON (Pinch) mode; d) all ribs ON (Clamp) mode. Different configurations can provide various stiffness for the gripper's finger to adapt the objects with different shapes and weights. To optimize the design, the stiffness analysis under various configurations and force conditions was implemented by finite element analysis (FEA). The 3-D printed prototypes were constructed to verify the feature and performance of the design concept of the VSG compared with the FEA results. The design of the VSG provides a novel idea for industrial robots and collaborative robots on adaptive grasping.

Keywords: Variable stiffness gripper · Fin Ray effect · Discrete stiffness change · Robotic grasping · Adaptive grasping

1 Introduction

Compared with traditional rigid manipulators, adaptive grippers are able to fulfill variable tasks in an unstructured environment. Most traditional rigid grippers are not compliant enough to grip deformable or delicate objects. Therefore, the expansion of soft and adaptive grippers would provide better solutions for the robotics field. Adaptive grippers are widely-used, both for industrial robots and collaborative robots [1].

Many solutions of adaptive grippers have been developed [2, 3] such as pneumatic 3D printed soft grippers [4], tendon-driven adaptive grippers [5–7], structural transformation based compliant variable stiffness grippers [8], Fin Ray grippers [9], etc. There are also a bunch of studies on the materials of grippers, for example, composites materials [10],

dielectric elastomer [11], memory alloy [12], and low-melting-point alloy [13]. Lots of innovative grippers with variable stiffness have also been proposed recently, they can adjust the stiffness by air-operated [14], magnetic [15], and rotating built-in elements [16, 17]. Additionally, there have been several excellent research publications on the characteristics, shape, structure, and parameters of Fin Ray [18–22].

Based on those ideas, this work will also introduce a novel variable stiffness gripper based on the Fin Ray effect that can adjust stiffness discretely. The main structure of the gripper includes the compliant frame, rotatable ribs, and the position limit components attached to the compliant frame. The stiffness of the gripper can be adjusted by rotating the specific ribs in the frame. This paper will focus on the mechanical design and performance of the VSG instead of building a mathematical model for fin ray structure which has been done by [23, 24].

The VSG can take into account both accuracy and speed, and it can grasp objects with a variety of hardness and shapes. For most soft grippers, it is difficult to ensure accuracy because of the low stiffness. In addition, the response speed of the VSG is very fast, as long as the motor drives the pulley to rotate, the stiffness can be changed rapidly in offline mode. Also, the VSG is low energy consumption. The servo motor only consumes power when the stiffness needs to be changed, but not when it is on standby. Third, the VSG has a simple structure and is easy to assemble. Its manufacturing cost is also low, and it is easy to replace if damaged.

The paper is structured as follows. Section 2 introduces the mechanical design of the VSG, and the concept implemented for adjusting the stiffness. Section 3 compares FEA and experiment data. Section 4 discusses the result and shows demos while Sect. 5 summarizes the work.

2   Concept of the Design

As shown in Fig. 1, the VSG is composed of two units: the driving mechanism and the grasping mechanism. The driving mechanism is used to realize the opening and tightening of the manipulator. The crank gear, rocker, and connecting rod constitute a parallelogram mechanism. The gear drive makes the two parallelogram mechanisms move synchronously. The motor transmits the rotation to the upper gear crank, which drives the movement of the two fingers. This is a common manipulator mechanism. The advantages of these mechanisms are simple and compact, which can achieve fast and precise control.

The overall structure of the grasping mechanism adopts the Fin Ray effect. The structure of the Fin Ray is a V-shaped frame with two bones on the sides and several ribs connected in between. For the VSG, the frame is designed as compliant, and the four ribs that support the frame have convertible angles, to realize discrete stiffness adjustment. The specific method is to connect two thin rods between the tip of the frame and the base to hold the ribs. The rod may increase the stiffness of the fingers, but it is designed to be as thin as possible and made of a compliant material to avoid interference with the overall stiffness as much as possible. Two belt pulleys are fixed on each rod, which is respectively connected with the upper two ribs and the lower two ribs through shafts. The pulley is connected to the servo motor through a belt. Each finger has 2 servo motors.

One motor controls the angular position of the lower two ribs, and the other controls the upper two ribs. In order to prevent the ribs from sliding and tilting to undesired angles, the ribs can be slidingly fitted into the grooves on the frame; this design is to prevent the ribs from sliding into other angles and causing unnecessary deflection in different rigid areas. When the servo motor is in the locked position, the ribs will be locked accordingly, and the locked movement will be transmitted to the pulley and ribs through the belt. Two fingers are defined as a synchronized configuration.
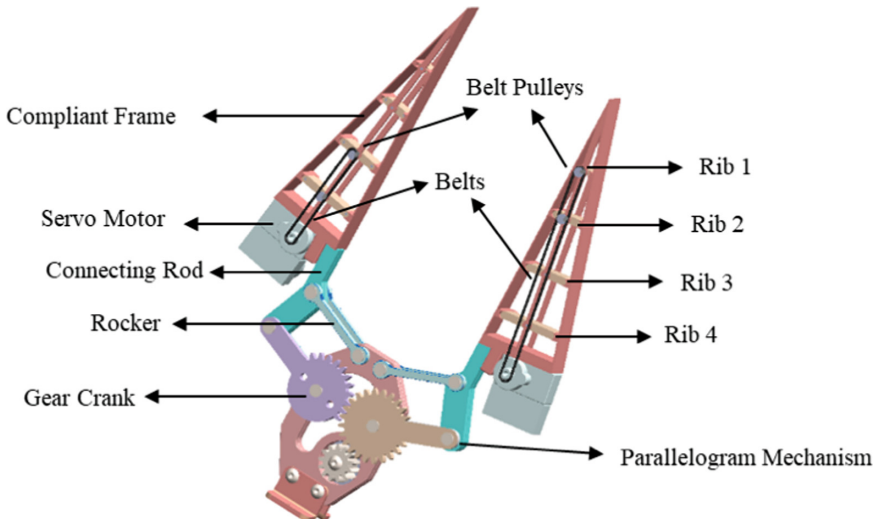
Fig. 1. 3-D model of the VSG.

Therefore, this mechanism has four configurations to achieve four stiffness levels to suit the objects with various hardness and dimension, as shown in Fig. 2. When all the ribs are out of contact with the frame, the system is in all ribs OFF status, also called Flex mode. This mode is suitable for grabbing larger soft objects or fragile objects. At this time, the priority of protecting items is higher than precision and speed. When the upper two ribs stay in contact with the frame and the lower two ribs leave the frame, the system is in upper ribs ON and lower ribs OFF status, also called Hold mode. This mode is suitable for grabbing heavy soft objects or fragile objects. The two fingers will wrap the object gently. When the upper two ribs leave the frame and the lower two ribs stay in contact with the frame, the system is in upper ribs OFF and lower ribs ON status, also called Pinch mode. This mode is suitable for grabbing light and small soft objects or fragile objects while ensuring high accuracy; when all ribs are in contact with the frame, the system is in all ribs on status, also called Clamp mode. This mode is suitable for grabbing hard objects with a variety of sizes, while the system is at high-speed operation to ensure maximum precision.

(a) Flex mode;(b) Hold mode; (c) Pinch mode; (d) Clamp mode.
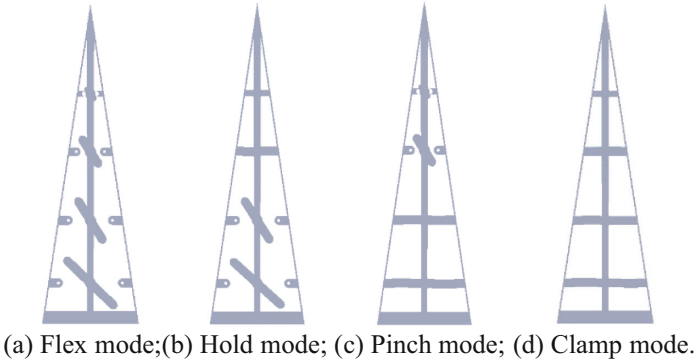
Fig. 2. Four configurations of the VSG.

A simple formula can be used to express the stiffness k_i of each rib i in different configurations, which is the ratio of force F to deflection δ_i:

$$k_i = \frac{F}{\delta_i} \tag{1}$$

3   FEA Simulation and Experimental Validation

3.1   Construction of the Prototype

According to the concept of design in Sect. 2, a prototype was constructed based on 3D printing. PLA was selected as the main material due to its high toughness and high strength characteristics. TPU 95A was not adopted in this case because the stiffness in Flex mode was too low to hold the object. When building the prototype, the design of the VSG was simplified, so pulleys and motors were not be installed. Therefore, pins are added between the two ends of the ribs and the compliant frame to prevent the ribs from being separated from the frame due to excessive force. This was to contrive the situation equivalent to the servo motor and the toothed pulley locking the ribs. This would allow ribs to rotate to a certain angle while force is being exerted and not to be separated from the frame. In 3D printing, the infill of the prototype was set to 40%, and the layer height was set to 0.1 mm.

3.2   Determination of Material Properties

The material properties of the same material under different printing configurations are different. The supplier did not provide the material properties of PLA at 40% infill, including density, Young's modulus, and Poisson's ratio. Measures were taken to obtain Young's modulus of our test specimen. According to the definition of Young's modulus, the longitudinal stress was divided by the strain, but the result was too small. A possible reason is that the 3-D printed parts are anisotropic, because of the different patterns and

infills when printing. Therefore, the deflection formula of the cantilever beam is used because it is the closest to the testing scenario:

$$\delta = \frac{FL^3}{3EI} \tag{2}$$

where L is the length of the beam; F is the force applied on one end of the beam; I is the moment of inertia of the beam; δ is the maximum deflection of the beam. The F and δ can be measured then substitute them to the equation to calculate E that is 3694 MPa. To make the results as accurate as possible, a cantilever beam with a size similar to one side frame and the same printing configuration was used, which is 200 × 1 × 2.4 mm. Moreover, we measured the density of PLA at 40% infill, and 0.1 mm layer height is 1.16 g/cm^3. In addition, Poisson's ratio has also been determined according to the negative of the ratio of transverse strain to axial strain, which is 0.39.

3.3 FEA Simulation

In order to evaluate the accuracy of our experiments on the prototype we created, FEA was used to implement static analysis of various force situations in ANSYS. A new PLA material was added to the engineering database, based on the parameters measured in Sect. 3.2. The simulation is to obtain 16 sets of deformation results for the four ribs under four configurations with a force ranging from 0 to 10N. As shown in Fig. 3, the animation ratio is 1:1. The parameters of the 3-D model used in the simulation are consistent with the prototype used in the experiment. The smallest deformation is in Clamp mode, when the probe exerts 10 N force on Rib 4, the deflection of Rib 4 is 0.29 mm. The largest deformation is in Flex mode, when the probe exerts 10 N force on Rib 3, the deflection of Rib 3 is 8.02 mm.

3.4 Experimental Validation

To verify the accuracy of the FEA simulation, experiments on the VSG were implemented. As shown in Fig. 4, a simplified 3-D printed VSG was fixed on a bench vise, and the bench vise was fixed on the leg of the experimental table. The Mark-10 M5-100 force gauge is installed on the ESM303 test stand and is used to measure the force applied on the ribs. The test stand has a travel display function, which can detect the deformation of the contact point. A flat tip shape probe was chosen because it would be best to simulate the actual force exertion onto the VSG when grasping an object. Then the probe was placed on the frame and the ribs were aligned. Next, we zeroed force and displacement and set the force threshold to 10N. The probe would then automatically press down until it reaches the threshold. These settings were the same as they were in ANAYS. To reduce the error, the experiment was repeated three times for 16 cases, and the results were averaged afterward.

(a) Flex mode;   (b) Hold mode;

(c) Pinch mode;   (d) Clamp mode.
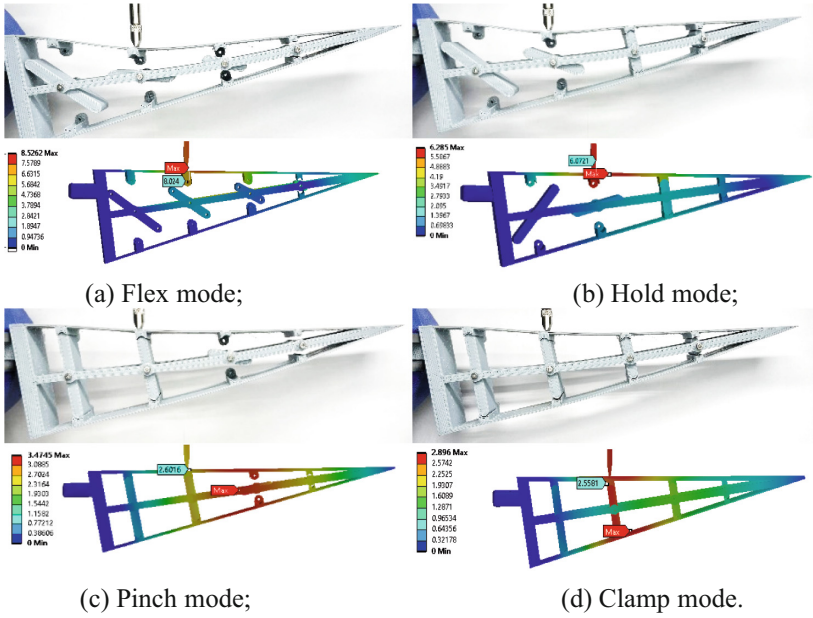
Fig. 3. The comparation between FEA simulation and experiment under different configurations on Rib 3.
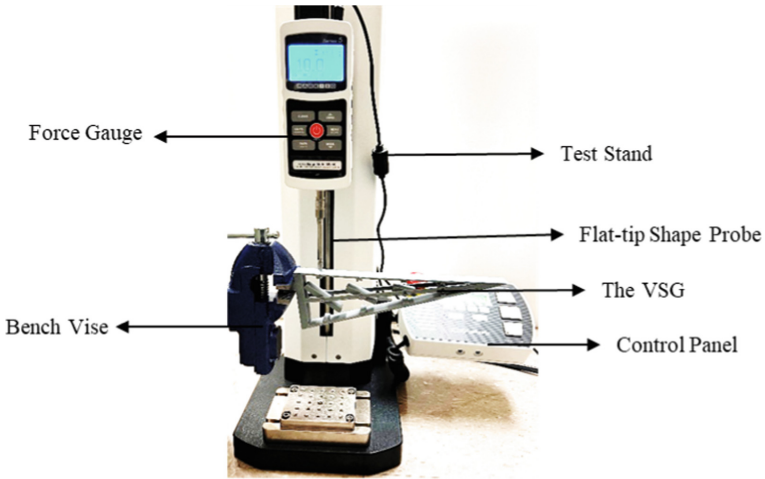
Fig. 4. Experimental setup.

**Table 1.** Main specifications of the VSG

| Parameters	Values	Units
Hight of the VSG	200	mm
Width of the VSG	60	mm
Thickness of the VSG	2.4	mm
The thickness of the compliant frame	1	mm
Weight of a VSG prototype	38	g
Peak load	40	N
Range of stiffness variation on Rib 4	4.13–33.33	N/m

4   Results

According to the FEA and experimental data, the comparison plots of different ribs under the same configuration were obtained, as shown in Fig. 5. Figure 5(a) shows the relationship between force and deflection of the four ribs in Flex mode. It could be seen that the deflection of all the ribs has reached the maximum level. Figure 5(b) presents the relationship between force and deflection of the four ribs in Hold mode. We can see the deflections of Ribs 1–3 are relatively large. Figure 5(c) shows the relationship between force and deflection of the four ribs in Pinch mode. The deflections of Rib 1–2 are relatively large here. Figure 5(d) shows the relationship between the force and deflection of the four ribs in Clamp mode. The deflections of all ribs are relatively small, especially Rib 4. In Hold mode and Pinch mode, the error of Rib 1 between the experimental values and FEA is relatively large, reaching 21%. One possible reason is the anisotropy caused by the different filling patterns of the 3-D printed parts, which can be accepted. The errors of other data are within 10%, This further proves the VSG design is feasible.

According to the FEA and experimental data, the comparison diagrams of the same stressed ribs under different configurations were obtained, as shown in Fig. 6. Figure 6(a) shows the relationship between force and deflection of Rib 1 in four configurations. Its stiffness variation range is very small, only 1.4 times the original stiffness. Figure 6(b) presents the relationship between force and deflection of Rib 2 in four configurations. Its stiffness variation range is also quite small, only 1.5 times. Figure 6(c) illustrates the relationship between force and deflection of Rib 3 in four configurations, and its stiffness variation range is moderate, which is 3 times. Rib 3 is the most commonly used position for grabbing objects in reality. Figure 6(d) shows the relationship between force and deflection of Rib 4 in four configurations. Its stiffness varies in a large range up to 8 times its original stiffness, but the deflection itself is not large enough.
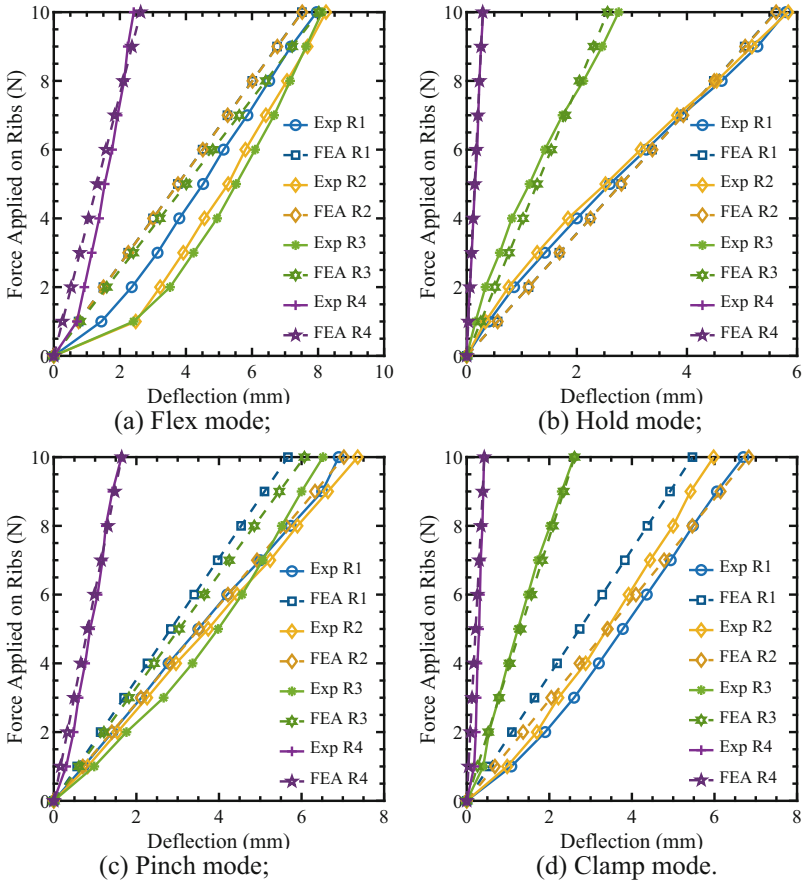
Fig. 5. Comparison between FEA simulation and experiment with different ribs under same configurations.

Figure 7 shows the comparison of maximum and minimum stiffness when the probe exerts a force on Rib 4 in FEA. Regardless of the position of the ribs and considering the global stiffness, the maximum stiffness of the VSG in Clamp mode is 11 times that in Flex mode.
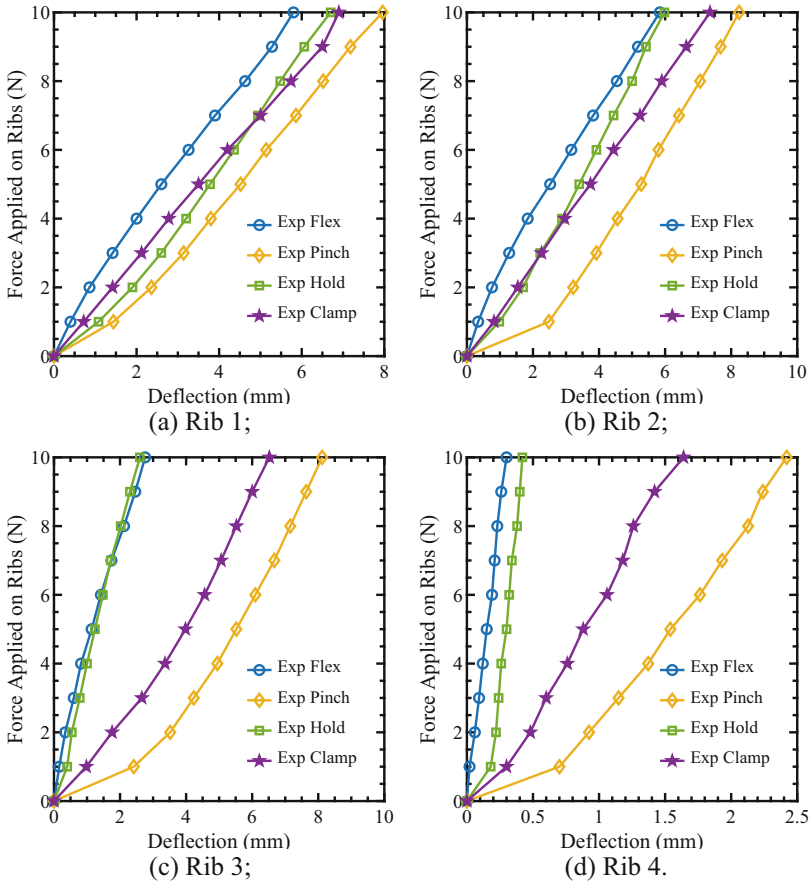
Fig. 6. Comparison the same ribs under different configurations based on experiment data.

The VSG can grab various objects in four configurations. Figure 8(a) shows the situation of the VSG grabbing a large piece of foam in Flex mode. In this case, the force required for this task is very small. Figure 8(b) illustrates the case of the VSG holding the paper cup in Hold mode where the deformation of the paper cup is inconspicuous. Figure 8(c) presents the situation of the VSG pinching the egg in Pinch mode, where the deformation of the frame is not large, and the egg is not crushed. Figure 8(d) shows the case where the VSG clamps the solid box in Clamp mode. It can be seen from the picture that the deformation of the frame is not obvious, and the box does not slip off. The demonstration of these demos proves that the design of the VSG is feasible.
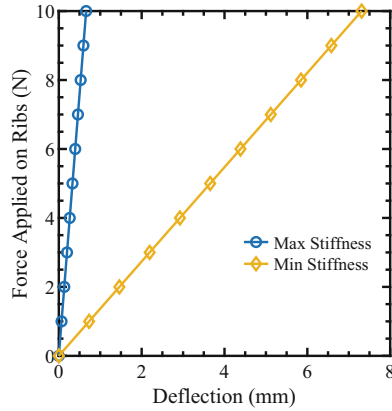
Fig. 7. FEA simulation under configurations of minimum and maximum stiffness.

(a) Flex mode;   (b) Hold mode;   (c) Pinch mode;   (d) Clamp mode.
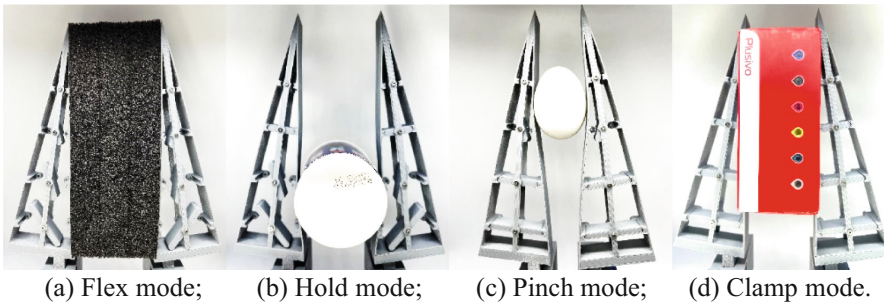
Fig. 8. Grasping of different objects by the VSG.

5   Conclusions

This paper proposes an innovative design concept of a variable stiffness gripper (VSG) based on the Fin Ray effect that can adjust its stiffness discretely for industrial robots and collaborative robots on adaptive grasping. The basic principle of this concept was to change the stiffness of a gripper of a fin ray design by allowing the ribs to rotate to allow such features to be realized. The ribs were divided into two sets of groups and there are four modes for our gripper design: the clamp, hold, pinch and flex modes. We measured the material properties of PLA in a specific configuration and imported it into FEA to simulate the deformation of the four ribs in different configurations. Also, a prototype was built, and our experimental results are in good agreement with the FEA. A grasp test was conducted to identify its ability to adapt objects with different sizes and hardness for better observation. The experiment was set to exert a 10 N force onto the gripper under 16 situations and the results matched our expectation of the FEA. Most of the results fell within a 10% range of difference from the FEA results, and it proves to achieve a maximum of 8 times change in stiffness compared to its original characteristics. Theoretically, the ribs would be operated by two servo motors through a belt and pulley

system to change their positions. We contrived this feature in our prototype and there would be further studies underway to improve its performance.

References

1. Muthusamy, R., Huang, X., Zweiri, Y., Seneviratne, L., Gan, D., Muthusamy, R.: Neuromorphic event-based slip detection and suppression in robotic grasping and manipulation. IEEE Access **8**, 153364–153384 (2020)
2. Huang, X., et al.: Neuromorphic vision based contact-level classification in robotic grasping applications. Sensors **20**, 4724. 20, 4724 (2020)
3. Wei, Y., et al.: A novel, variable stiffness robotic gripper based on integrated soft actuating and particle jamming. Soft Robot. **3**, 134–143 (2016)
4. Zhang, P., Chen, W., Tang, B.: Design and feasibility tests of a lightweight soft gripper for compliant and flexible envelope grasping (2021). https://home.liebertpub.com/soro
5. Al Abeach, L.A.T., Nefti-Meziani, S., Davis, S.: Design of a variable stiffness soft dexterous gripper. Soft Robot. **4**, 274–284 (2017)
6. Hussain, I., et al.: Compliant gripper design, prototyping, and modeling using screw theory formulation: Int. J. Robot. Res. **40**, 55–71 (2020). https://doi.org/10.1177/0278364920947818
7. Chen, R., et al.: Bio-inspired shape-adaptive soft robotic grippers augmented with electroadhesion functionality. Soft Robot. **6,** 701–712 (2019). https://home.liebertpub.com/soro
8. Hussain, I., et al.: Modeling and prototyping of an underactuated gripper exploiting joint compliance and modularity. IEEE Robot. Autom. Lett. **3**, 2854–2861 (2018)
9. Hussain, I., et al.: Design and prototype of supernumerary robotic finger (SRF) inspired by fin ray® effect for patients suffering from sensorimotor hand impairment. RoboSoft 2019–-2019 .In: EEE International Conference on Soft Robot, pp. 398–403 (2019)
10. Hussain, I., et al.: Design and prototyping soft–rigid tendon-driven modular grippers using interpenetrating phase composites materials: Int. J. Robot. Res. **39**, 1635–1646 (2020). https://doi.org/10.1177/0278364920907697.
11. Yang, Y., Chen, Y., Li, Y., Wang, Z., Li, Y.: Novel variable-stiffness robotic fingers with built-in position feedback. Soft Robot. **4**, 338–352 (2017)
12. Wang, W., Ahn, S.H.: Shape memory alloy-based soft gripper with variable stiffness for compliant and effective grasping. Soft Robot. **4**, 379–389 (2017). https://home.liebertpub.com/soro
13. Hao, Y., et al.: A variable stiffness soft robotic gripper with low-melting-point alloy. In: Chinese Control Conference CCC, pp. 6781–6786 (2017)
14. Arachchige, D.D.K., Chen, Y., Walker, I.D., Godage, I.S.: A novel variable stiffness soft robotic gripper. In: International Conference on Automation Science and Engineering, 2021-August, pp. 2222–2227 (2020)
15. Memar, A.H., Mastronarde, N., Esfahani, E.T.: Design of a novel variable stiffness gripper using permanent magnets. In: Proceedings of International Conference on Robotics and Automation, pp. 2818–2823 (2017)
16. Li, X., Chen, W., Lin, W., Low, K.H.: A variable stiffness robotic gripper based on structure-controlled principle. IEEE Trans. Autom. Sci. Eng. **15**, 1104–1113 (2018)

17. Chandrasekaran, K., Somayaji, A., Thondiyath, A.: A novel design for a compliant mechanism based variable stiffness grasper through structure modulation. J. Med. Devices Trans. ASME **15**, (2021)
18. Yang, Y., Jin, K., Zhu, H., Song, G., Lu, H., Kang, L.: A 3D-printed fin ray effect inspired soft robotic gripper with force feedback. Micromachines **12**, 1141. 12, 1141 (2021)
19. Basson, C.I., Bright, G.: Geometric conformity study of a fin ray gripper utilizing active haptic control. In: International Conference on Control, Automation ICCA. 2019-July, pp. 713–718 (2019)
20. Elgeneidy, K., Lightbody, P., Pearson, S., Neumann, G.: Characterising 3D-printed soft fin ray robotic fingers with layer jamming capability for delicate grasping. RoboSoft 2019 2019. In: IEEE 4th International Conference on Soft Robotics, pp. 143–148 (2019)
21. Elgeneidy, K., Fansa, A., Hussain, I., Goher, K.: Structural optimization of adaptive soft fin ray fingers with variable stiffening capability. In: 2020 3rd IEEE International Conference on Soft Robotics (RoboSoft), pp. 779–784 (2020)
22. Ali, M.H., Zhanabayev, A., Khamzhin, S., Mussin, K.: Biologically inspired gripper based on the fin ray effect. In: 2019 5th International Conference on Control, Automation and Robotics, ICCAR 2019, pp. 865–869 (2019)
23. Armanini, C., Hussain, I., Iqbal, M.Z., Gan, D., Prattichizzo, D., Renda, F.: discrete cosserat approach for closed-chain soft robots: application to the fin-ray finger. IEEE Trans. Robot. **37**, 2083–2098 (2021)
24. Anwar, M., Khawli, T. Al, Hussain, I., Gan, D., Renda, F.: Modeling and prototyping of a soft closed-chain modular gripper. Ind. Rob. **46**, 135–145 (2019)